Growth and Deformation of the Ladakh Batholith, Northwest Himalayas: Implications for Timing of Continental Collision and Origin of Calc-Alkaline Batholiths

Roberto F. Weinberg[1] *and W. J. Dunlap*

Research School of Earth Sciences, Australian National University, Australian Capital Territory 0200, Australia (*e-mail: rweinber@geol.uwa.edu.au*)

ABSTRACT

The calc-alkaline Ladakh batholith (NW Himalayas) was dated to constrain the timing of continental collision and subsequent deformation. Batholith growth ended when collision disrupted subduction of the Tethyan oceanic lithosphere, and thus the youngest magmatic pulse indirectly dates the collision. Both U-Pb ages on zircons from three samples of the Ladakh batholith and K-Ar from one subvolcanic dike sample were determined. Magmatic activity near Leh (the capital of Ladakh) occurred between 70 and 50 Ma, with the last major magmatic pulse crystallizing at ca. 49.8 ± 0.8 Ma (2σ). This was followed by rapid and generalized cooling to lower greenschist facies temperatures within a few million years, and minor dike intrusion took place at 46 ± 1 Ma. Field observations, the lack of inherited prebatholith zircons, and other isotopic evidence suggest that the batholith is mantle derived with negligible crustal influence, that it evolved through input of fresh magma from the mantle and remelting of previously emplaced mantle magmatic rocks. The sedmimentary record indicates that collision in NW Himalaya occurred around 52–50 Ma. If this is so, the magmatic system driven by subduction of Tethys ended immediately on collision. The thermal history of one sample from within the Thanglasgo Shear Zone (TSZ) was determined by Ar-Ar method to constrain timing of batholith internal deformation. This is a wide dextral shear zone within the batholith, parallel to the dextral, N 30° W–striking crustal-scale Karakoram Fault. Internal deformation of the batholith, taken up partly by this shear zone, has caused it to deviate from it regional WNW-ESE trend to parallel the Karakoram Fault. Microstructures and cooling history of a sample from the TSZ indicate that shearing took place before 22 Ma, implying that (1) the history of dextral shearing on NW-striking planes in northern Ladakh started at least 7 m.yr. before the <15 Ma Karakoram Fault, (2) shearing was responsible for deviation of the regional trend of the Ladakh batholith, and (3) dextral shearing occured within a zone apporximately 100 km wide that includes the Ladakh batholith and portions of the younger Karakoram batholith.

Introduction

The Ladakh batholith (NW Himalayas, India) is part of the Andean-type, Trans-Himalayan (Gangdese) Plutonic Belt that extends for 2500 km from Afghanistan in the west (the Kohistan batholith) to east of Lhasa in Tibet (fig. 1; Honegger et al. 1982; Schärer et al. 1984*a*). It is composed of multiple calc-alkaline intrusions that vary in composition from olivine-norite and gabbro to granite (Honegger et al. 1982). The batholith trends roughly WNW, is approximately 600 km long and 30–50 km wide, and is believed to have had a similar developmental history to that of the Kohistan batholith to the west. Both batholiths are sandwiched between the Indus Suture Zone to the south, a result of the continental collision between India and Eurasia, and the Shyok Suture Zone to the north, a result of an earlier collision between the Ladakh (and Kohistan) block and the southern margin of Eurasia.

The two batholiths resulted from melting related to the north-directed subduction of the Tethyan oceanic crust (e.g., Schärer et al. 1984*a*) below an island arc situated along the southern margin of Eurasia. A large sliver of sedimentary rocks within

Manuscript received June 23, 1999; accepted January 6, 2000.

[1] Current address: Centre for Strategic Mineral Deposits, Department of Geology and Geophysics, University of Western Australia, Nedlands, Western Australia 6907, Australia.

[The Journal of Geology, 2000, volume 108, p. 303–320] 0022-1376/2000/10803-0003$01.00

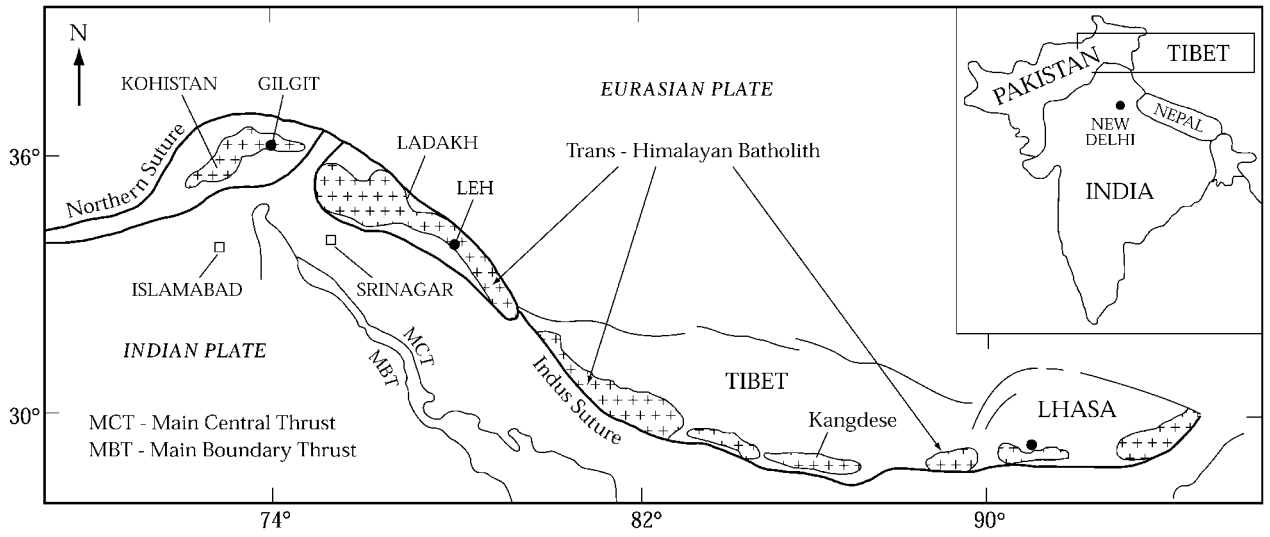

Figure 1. The Trans-Himalayan Plutonic Belt extending from the Kohistan batholith in the west to Lhasa in Tibet and beyond in the east (redrawn from Petterson and Windley 1991).

the Ladakh batholith led Raz and Honegger (1989) to suggest that it may have developed in a transitional environment between the Kohistan island arc in the west and the continental margin of Eurasia in the east. The few known crystallization ages of Ladakh granitoids (102 and 60–62 Ma; Honegger et al. 1982; Schärer et al. 1984*a*) indicate that magmatic activity preceded continental collision between Eurasia and India and ended roughly at the time collision started between 60 and 50 Ma (e.g., Schärer et al. 1984*a*; Beck et al. 1995). This suggests that collision shut off magmatism in Ladakh by disrupting (decelerating and steepening) the subduction of Tethys.

The general NW-SE trends of the Ladakh and Karakoram batholiths in northern Ladakh display a large-scale clockwise bend in the vicinity of the dextral Karakoram Fault (fig. 2; De Terra 1934, p. 26–28). The clockwise rotation of the Ladakh and Karakoram batholiths away from their regional trends, south and north of the fault, respectively, suggests that they have undergone internal deformation to accommodate dextral movement. The N 30° W–trending Karakoram Fault is one of the main structures bounding the southwest edge of the Tibetan Plateau and is thought to control its eastward extrusion (Tapponier et al. 1982). However, Searle et al. (1998) and Weinberg et al. (2000) demonstrated that the Karakoram Fault was initiated after intrusion of the Karakoram leucogranite between 18 and 15 Ma and displaced rocks on either side by a maximum of 150 km. To understand and constrain this internal deformation, the newly found Thanglasgo Shear Zone (TSZ) in the northern part of the Ladakh Batholith was studied.

This article reports on regional structural observations and dating of samples from a 30-km-wide, N-S band across the Ladakh batholith and derives the history of batholith growth and deformation. To understand the magmatic evolution of the batholith and help constrain the time of collision, U-Pb zircon dating of three granitoid samples from the batholith was carried out using SHRIMP II. In addition, one Ar-Ar step heating experiment was performed on a hornblende separate from a subvolcanic dike. To understand the timing of internal dextral shearing of the Ladakh batholith, another Ar-Ar step heating experiment on a K-feldspar sample from the TSZ was carried out. We discuss the results in terms of the origin of calc-alkaline batholiths; timing of continental collision; and regional, collision-related deformation.

Age and Origin of the Ladakh Batholith: Previous Work

Ladakh Batholith magmatic rocks have yielded 102 ± 2 Ma U-Pb ages near Kargil (west of Leh) and a 60 ± 5 Ma Rb-Sr whole rock isochron age around Leh (table 1; Honegger et al. 1982; Schärer et al. 1984*a*). Biotite from near Leh yielded a K-Ar age of 48.7 ± 1.6 Ma (Honegger et al. 1982), suggesting significant cooling of the igneous rocks by that time. In addition, crystallization ages of Ladakh

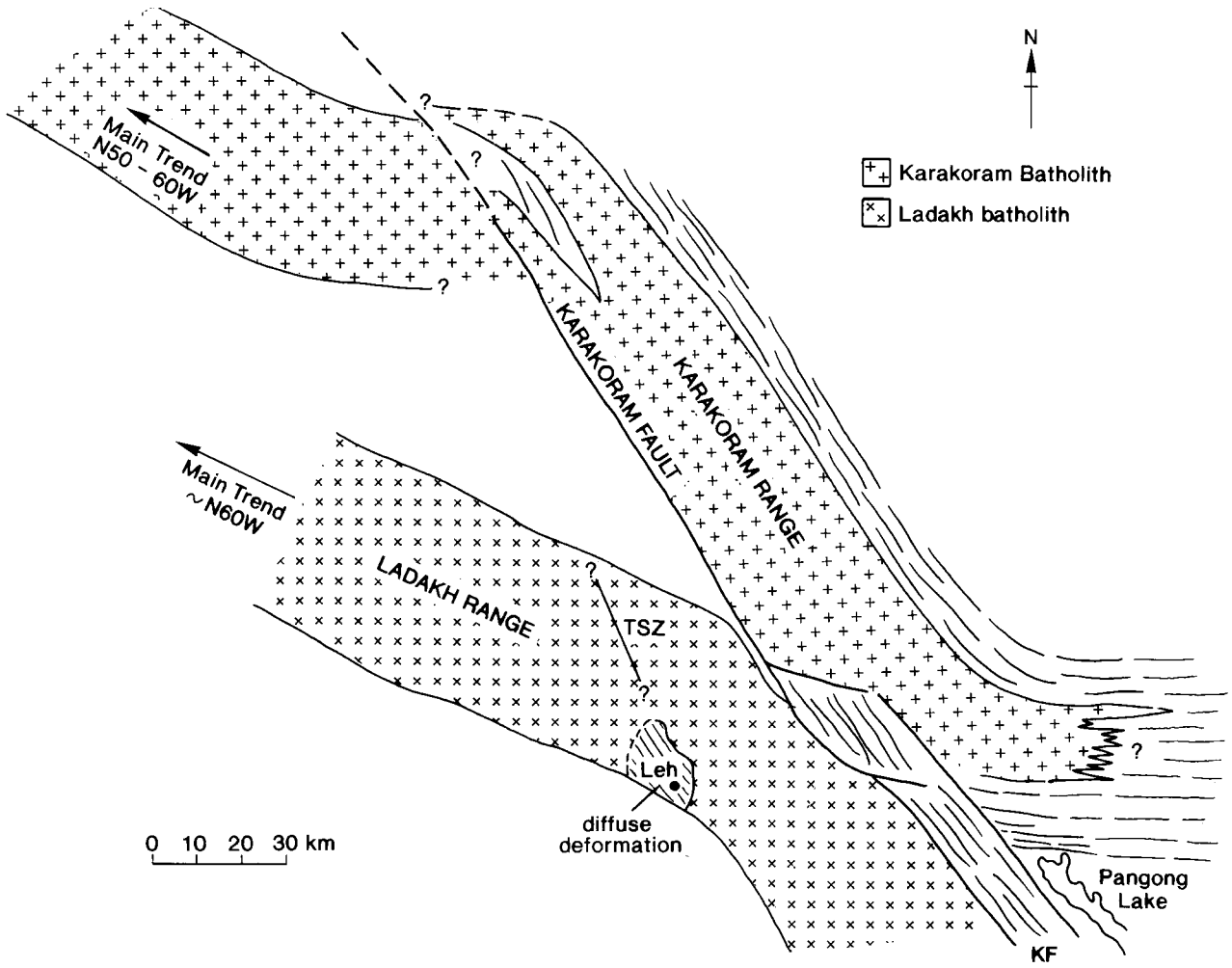

Figure 2. Schematic map of the bend on the main trends of the Ladakh and Karakoram batholiths as they approach the Karakoram Fault (see fig. 3 for location).

plutons broadly coincide with Rb-Sr ages (whole rock isochrons) from Kohistan (Petterson and Windley 1985; George et al. 1993). In Kohistan, however, a postcollisional age has also been determined for leucogranite sheets.

Restricted participation of older continental crust in the building of the Ladakh and Kohistan batholiths has been suggested by $\delta^{18}O$ studies (Blattner et al. 1983; Debon et al. 1986; Srimal et al. 1987). Initial $^{87}Sr/^{86}Sr$ ratios between 0.7033 and 0.7053 (recalculated from the values of Honegger et al. 1982 and Srimal 1986), using granitoid ages of 103 Ma for western Ladakh and 60 Ma for eastern Ladakh, suggest an origin from an undepleted mantle (Allègre et al. 1983) with insignificant participation of older crust (a wider spread in values is to be expected if older crust has contributed to batholith growth).

On the basis of multigrain analyses, Schärer et al. (1984*a*) found that zircons from the Ladakh granite (near Leh) were discordant, suggesting that some zircons had inherited radiogenic Pb from older (at least 350–590 Ma) continental crust. Schärer et al. (1984*a*) argued that Allègre and Ben Othman's (1980) Ladakh granodiorite sample (HB68) carried a Nd isotope signature of magma derived from Late Proterozoic basement. Here, we suggest an alternative interpretation: (1) Allègre and Ben Othman presented Sm-Nd data for two samples of the batholith (HB68 and HB74). The $^{143}Nd/^{144}Nd$ ratio for both samples become identical within error when corrected by ^{147}Sm decay back to 51 Ma (the age of intrusion quoted), indicating that the samples are cogenetic and approximately 50 m.yr. old. (2) Model ages relative to different depleted mantle models vary from 720 to 800 Ma for HB68 (similar to the

Table 1. Summary of Geochronological Data Reflecting Crystallization Ages for the Ladakh and Kohistan Batholiths

Batholith	Ma
Ladakh:	
Leh	45.7 ± 0.8 hornblende Ar-Ar[a]
	48.7 ± 1.6 biotite K-Ar [b]
	49.8 ± 0.8 zircon U-Pb[a]
	58.4 ± 1.0 zircon U-Pb[a]
	61.5 ± 2.0 zircon U-Pb[a]
	63 ± 5 zircon U-Pb[c]
	60–62 allanites and monazites, U-Pb[c]
	60 ± 10 Ma, Rb-Sr[a]
Kargil	101 ± 2 Ma, U-Pb[c]
	103 ± 3 Ma, U-Pb[b]
Kohistan	26 ± 1 Rb-Sr [d]
	49 ± 11 Rb-Sr [d]
	54 ± 4 Rb-Sr[e]
	102 ± 12 Rb-Sr[e]

Note. Kargil is 250 km west of Leh.
[a] This work.
[b] Honegger et al. (1982).
[c] Schärer et al. (1984*a*).
[d] George et al. (1993).
[e] Petterson and Windley (1985).

model age in Schärer et al. 1984*a*) and −200 to −300 Ma for HB74. Schärer et al. (1984*a*) chose to ignore the future model age of sample HB74 and focused on the Late Proterozoic model age for HB68, although there is no reason to exclude either of the samples. The large, depleted model age dispersion (ca. 1 Ga between the two samples) could possibly result from different degrees of fractionation of the two samples (cumulates are common, and allanite is a common mineral in Ladakh granitoids); it could also mean that the melt was not derived from such a depleted source. (3) A derivation from mantle with near-chondritic isotope ratios (as indicated by the identical CHUR model ages) is supported by the limited range of $^{87}Sr/^{86}Sr$ initial values around 0.704. Unless it is coincidental that the two samples form a two-point isochron with approximately their known age, Sm-Nd systematics supported by Sr isotope ratios suggest that the Ladakh batholith was derived from mantle with near-chondritic isotope ratios.

Plutonic rocks from the Kohistan batholith have yielded similar initial Sr ratios (0.7039–0.7050; Petterson and Windley 1985), and positive ϵ_{Nd} values indicate a short, 60–70 m.yr., crustal residence time (Petterson et al. 1993). Petterson et al. (1993) found no evidence in Kohistan for the participation of older crust in the growth of the batholith. In summary, the few age determinations for the Ladakh batholith constrain magmatic activity to between 103 and ca. 60 Ma, followed by rapid cooling. Whereas participation of older continental crust has been suggested by discordant zircons, initial Sr ratios, Sm-Nd isotopes, and the island arc setting suggest that these granitoids were derived from the mantle, most likely through an intermediate stage of short residence in the lower crust.

Ladakh Batholith: Geochronology

Recent detailed mapping of the Ladakh batholith around the town of Leh revealed two plutons, the older, composite Gyamsa pluton and the younger Leh pluton. Where the two plutons are in contact, granites and diorites of the Leh pluton intrude the Gyamsa pluton. The Leh pluton, which grades from diorite to granite, is intruded in turn by late-magmatic leucogranite dikes (Shey granite, fig. 3*B*; Weinberg 1997). There is a still younger igneous event characterized by the intrusion of andesitic and rhyolitic dikes that cuts rocks of the Leh pluton. These dikes were only found west of the village of Phyang (fig. 3*B*) and are referred to here as the Phyang dikes. They are a minor addition to the total volume of the pluton, and their subvolcanic textures indicate rapid cooling.

The Gyamsa migmatite complex and pluton are grouped here under a single term, the Gyamsa pluton, which has migmatite on its western side and a pluton formed by segregated melt products (mafic-poor tonalites, granodiorites, and granites) to the east (fig. 3*B*). The migmatite resulted from the partial melting of an amphibolite of quartz-diorite composition (57%–62% SiO_2). The igneous origin of the amphibolite is indicated by zoned plagioclase phenocrysts. A range of melting stages of the amphibolite is preserved: from the unmelted, more refractory parts of the amphibolite; to stromatic migmatites; to larger, meter-scale heterogeneous magma blobs within migmatites; to even larger, heterogeneous magma bodies with disaggregated pieces of the source amphibolite. The stromatic migmatites have narrow (centimeter-wide) bands of melanosomes and leucosomes partly drained by crosscutting dikes, as suggested by flow structures preserved by partly disaggregated melanosomes.

Two samples from the Leh pluton (samples 020 and 018, fig. 3*B*), as well as a third sample from the northern margin of the batholith, were dated by SHRIMP II. The last was collected close to the village of Digar (sample 019, fig. 3*A*) and should indicate age trends across the main strike of the batholith. We also determined the age of a hornblende sample extracted from an andesitic Phyang dike by means of $^{40}Ar/^{39}Ar$ analysis.

Leh Pluton—Sample 018. This sample, collected

9 km east of Leh (2 km east of the village of Sobu, fig. 3*B*), is a medium-grained quartz-diorite (color index of 20–30) with zoned andesine, partly chloritized biotite and hornblende, augite partly substituted by hornblende and interstitial quartz and minor orthoclase (untwinned) and with sphene, opaques, zircon, apatite, and epidote as accessories. This rock type was intruded by the Shey leucogranite at late stages of crystallization when both magmas mingled (Weinberg 1997).

This sample has two main zircon varieties as depicted on cathodoluminescence images (fig. 4*A*, 4*B*): a finely zoned, stubby phase (aspect ratio 2–3) with a later overgrowth truncating core zonation and a homogeneous, high-U, and needle-shaped phase (aspect ratio 3–6). Two other minor varieties were found: (1) needle-shaped (aspect ratio of circa 4) but with low U content and (2) amorphous zircons. Only one zircon of each of these two minor varieties were dated (types 3 and 4 in table 2, respectively). The morphology and internal zoning patterns of the needle-shaped and stubby zircons of the main population indicate that they have an igneous origin. These zircon phases yielded two distinct U^{206}/Pb^{238} ages (table 2 and fig. 4*C*; tables 2–6 are available from *The Journal of Geology* Data Depository on request). The stubby zircons yielded a mean weighted age of 58.1 ± 1.6 Ma (2σ), and the needle zircons were dated at 49.8 ± 0.8 Ma (2σ). The age of the thin overgrowth around the stubby zircons was analyzed in one zircon only (fig. 4*A*) and yielded an age similar to that of the younger zircon phase (50.0 ± 1.3 Ma, spot 14.2, table 2). The zircons of the two minor varieties yielded ages similar to those of the two other groups and were therefore grouped with them (spots 4.1 and 6, table 2).

The younger group has higher U and Th contents than the older group. The possibility of high U levels having affected the apparent calculated ages has been eliminated by checking for any systematic correlation between U content and age within each group, and by noting that zircons of similar U content are present in both groups (e.g., spots 8.1 and 2.1, table 2). Most $^{208}Pb/^{232}Th$ and $^{206}Pb/^{238}U$ analyses yielded similar ages within error (fig. 4*D*), lending confidence to the analytical method and suggesting that the U-Th-Pb system was essentially closed. Larger errors in Th-ages (caused by low ^{208}Pb content) do not allow statistical discrimination of the two age groups determined by $^{206}Pb/^{238}U$.

A χ^2 test for U-Pb ages of all spots, independent of any grouping, yields a very high value, indicating that the sample population does contain more than one age group. After dividing the population into the two smaller groups, the χ^2 value was still relatively high, suggesting that either the number of data points is insufficient to characterize a Gaussian distribution or that each group should be further divided. The latter case is unlikely because each age group is confined to a single zircon morphology. Thus, more data points would most likely improve precision of the results but not change their essence.

We interpret the needle-shaped zircons and the rim overgrowth of the stubby zircons as new growths dating the crystallization of the quartz-diorite, while the older stubby zircons are inherited from the source and define the crystallization age of the source igneous rock. The Leh Pluton (including the Shey granite) is the youngest main magmatic pulse in this area, and its 49.8 ± 0.8-Ma crystallization age is contemporaneous with the end of suturing of India to the southern margin of Eurasia. The age coincidence between continental collision and the last major calc-alkaline magma pulse (Leh Pluton) suggests collision interrupted magmatism by disrupting subduction of the Tethys oceanic lithosphere.

Gyamsa Migmatite—Sample 020. A xenolith of migmatitic amphibolite from within the Leh pluton was dated (fig. 3*B*). This xenolith has a texture and mineralogy similar to migmatites of the Gyamsa pluton, and its trace elements and REE contents are also similar to those of Gyamsa rocks (high Nb and Yb and low Sr/Y) and very distinct from samples of the Leh pluton (P. Sylvester, unpub. data). Partial melting of the amphibolite occurred before intrusion of the 49.8 ± 0.8-Ma Leh magma (sample 018) as indicated by crosscutting relationships.

The leucosomes of the analyzed sample are felsic and have a few plagioclase phenocrysts (up to 0.7 mm long) with lamellar twinning in a fine matrix (0.1–0.4 mm) of plagioclase, perthitic orthoclase, quartz, and minor green to light-brown biotite. The melanosome has yellow to brown biotite and approximately 40% of green hornblende in the mode. The accessory minerals of both melanosome and leucosome are zircon, sphene, apatite, and large epidote. Zircon grains are small (50–100 μm; fig. 5*A*, 5*B*) and similar in size and shape in both melanosomes and leucosomes. They may be found either as isolated grains or as aggregates, and some are found within melanosome biotite. Some show zoned cores truncated and overgrown by thin rims (fig. 5*A*, 5*B*). Zircon grains are of similar size and show fine, prismatic zoning. These observations indicate that zircon was present in the original quartz-diorite and was inherited by the Gyamsa leucosome melts. The narrow rims may have

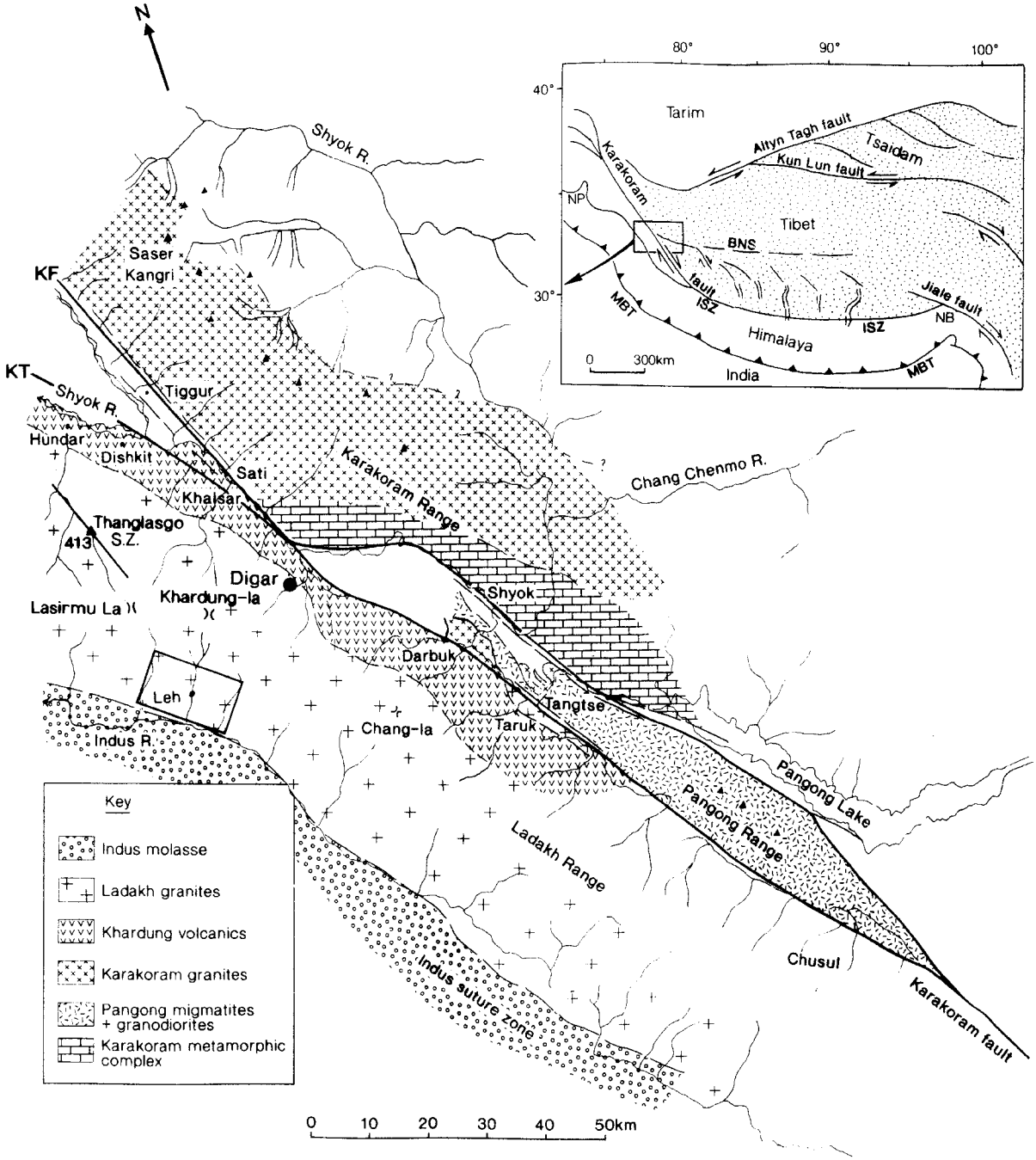

Figure 3A

Figure 3. *A*, Regional map of the Ladakh and Karakoram batholiths separated by the Karakoram Thrust (KT) and the Karakoram Fault (KF) (modified after Searle et al. 1998). The dextral Thanglasgo Shear Zone (TSZ) is parallel to the <15-Ma dextral Karakoram Fault. Sample 413 was collected from within this shear zone. The dot near the village of Digar shows the position of sample 019. Box around Leh indicates the position of (*B*). *B*, Geological map of the Leh and Gyamsa plutons (a thick line separates them). Areas mapped as Shey granite represent areas in which granite dominates over other rock types. In these areas sheets tend to coalesce to form large bodies. Areas mapped as migmatites are underlain by partially melted amphibolites and pools of heterogeneous anatectic melts. Location of samples 018 and 020 as indicated.

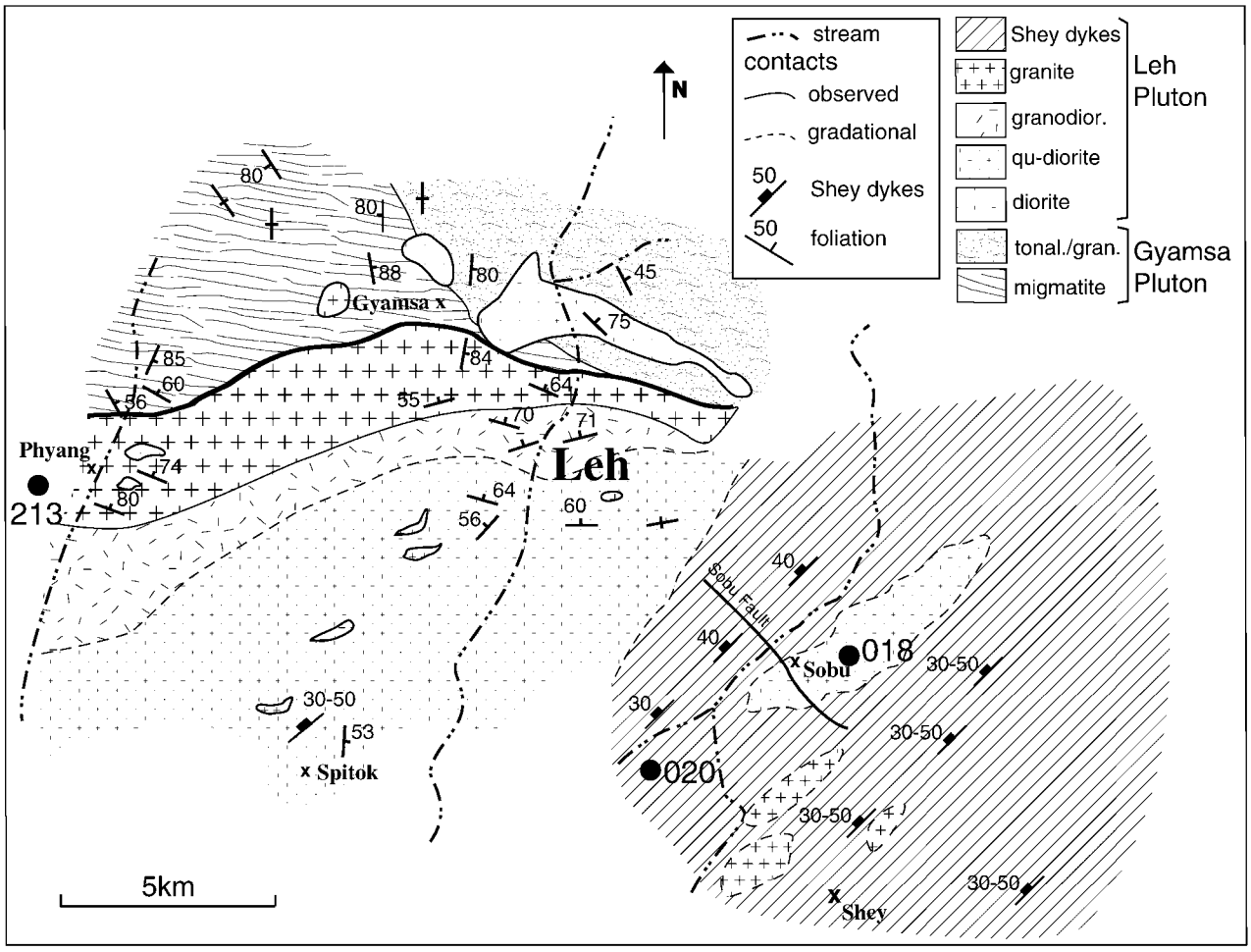

Figure 3B

grown during the partial melting episode, but it seems that no new zircon grains crystallized from this melt.

SHRIMP age determinations (table 3) show a variation in $^{206}Pb/^{238}U$ ages between 73 and 50 Ma, with one younger outlier (fig. 5*C*). The age range is well fitted by a single Gaussian distribution centered at 61.5 ± 2.0 Ma (2σ). These results are similar to the age range covered by $^{208}Pb/^{232}Th$ ages (table 3), but the latter have a very large error because of their low Th content. In a few analyses, a narrower beam was used to date narrow rim zones (marked with an asterisk in table 3); the same age range was found as for zircon interiors. This could result from a combination of rim overgrowth age indistinguishable, within error, from that of grain interiors and a beam that overlapped the two zones, obscuring any age difference.

Because zircon was present in the original Gyamsa quartz-diorite and later inherited by its melt products, and because these melts are older than the 49.8 ± 0.8-Ma Leh pluton, the two most likely interpretations of the results are that (1) the age spread includes the crystallization age of both the original quartz-diorite and its melt products or (2) that the age represents the time of crystallization of the original quartz-diorite, and its later remelting did not give rise to significant zircon growth. In either case, crystallization of the quartz-diorite closely precedes its later remelting and crystallization of its melt products. It is highly unlikely that all the igneous zircons in the original quartz-diorite were replaced during migmatization, but it is possible that the age represents the time of crystallization of the melt products, and the age of the quartz-diorite remains unknown.

Digar Granite—Sample 019. The Digar granite is a pink, coarse-grained, felsic granite (color index <5) with undeformed quartz, mesoperthitic K-feldspar, twinned plagioclase, partly chloritized biotite,

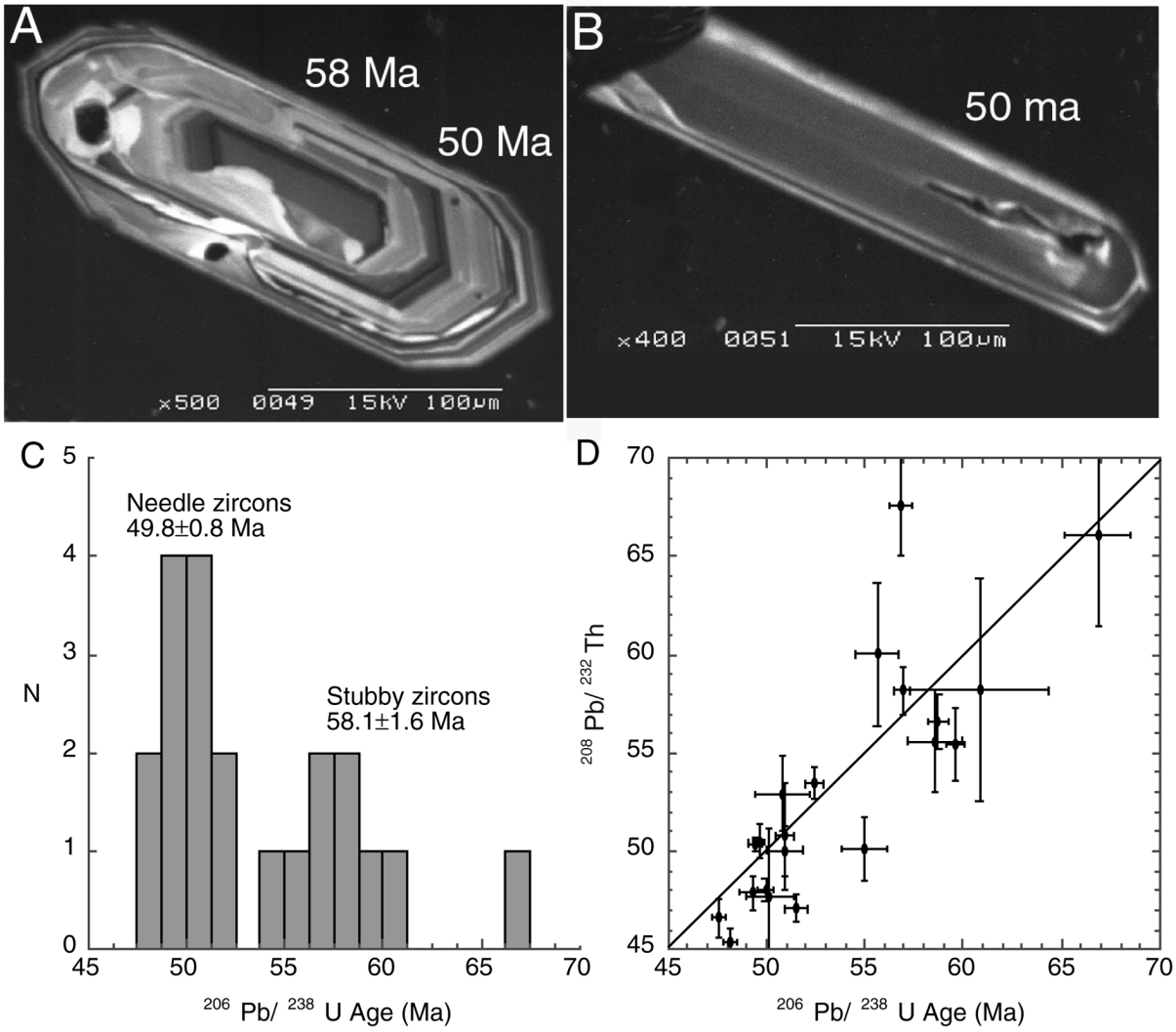

Figure 4. Cathodoluminescence images of two zircon grains, (*A*) zircon 14 and (*B*) zircon 3 (see table 3), representing the two main zircon morphologies in sample 018. The ages indicated correspond to the mean age for each morphological group. *C*, Histogram of zircon $^{206}Pb/^{238}U$ ages of sample 018 showing two age groups that coincide with the two main zircon morphologies; the cores of stubby zircons yield an age of ca. 58.1 ± 1.6 Ma, and the needle-shaped zircons and the one spot on the rim of a stubby zircon (*A*) yield 49.8 ± 0.8 Ma. *D*, Comparison between $^{206}Pb/^{238}U$ and $^{208}Pb/^{232}Th$ ages showing that, with a few exceptions, analyses yield the same age within error.

hornblende, sericite, sphene, and zircon. It crops out near the northern margin of the batholith a few hundred meters from the first outcrop of subvolcanic granophyric rock and close to the village of Digar (fig. 3*A*).

Analyses of 18 spots from sample 019 yielded a single mean age centered at 58.4 ± 1.0 Ma (2σ; table 4 and fig. 6), identical to the older group determined in sample 018. The analyses close to the central age have small errors and similar Th-Pb ages (fig. 6*b*). The oldest spot yielded an age of ca. 70 Ma (spot 8.2) and was excluded partly because of its distance from the mean age and partly because of its very different Th age (see table 4).

Phyang Dikes—Sample 213. The Phyang dikes crop out west of Phyang (fig. 3*B*). The exposed dike swarm represents a small volume of magma (tens of dikes in total), with dike widths varying between 1 cm and 6 m (generally between 50 cm and 1.5 m), with the entire swarm restricted to a few square kilometers. The dikes generally strike N 50°–70° E and dip between 70° SE and vertical. Dike composition is variable, as indicated by changes in phenocryst content: some dikes have embayed idio-

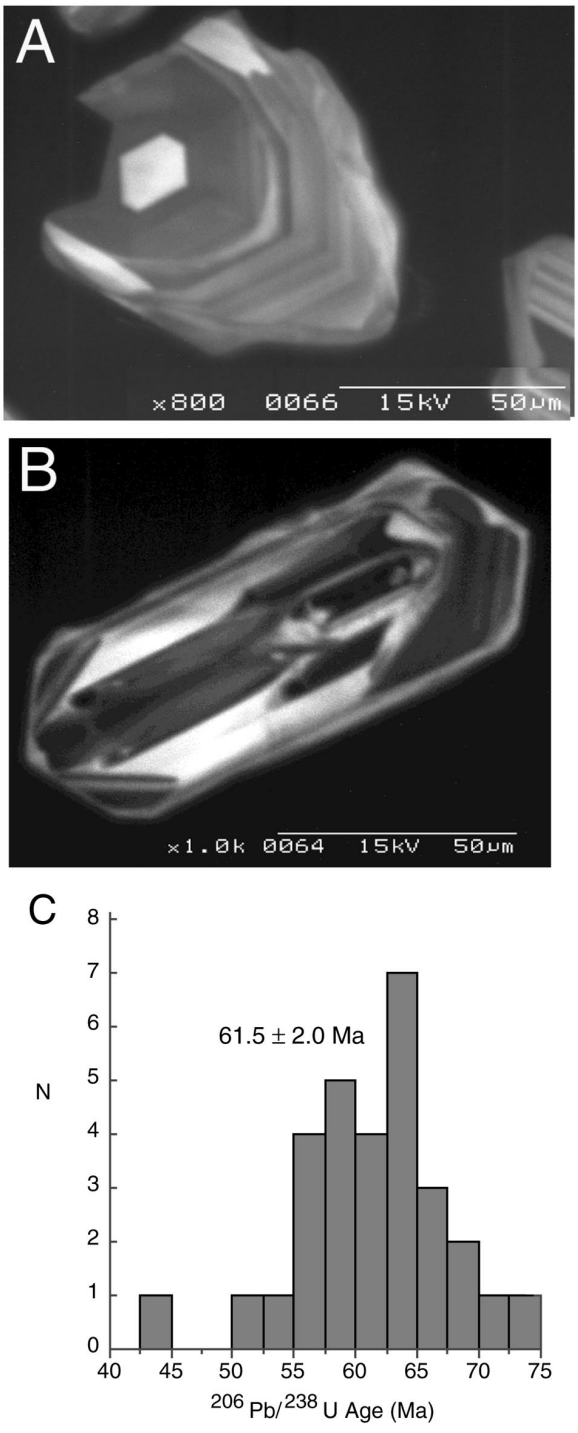

Figure 5. Cathodoluminescence images of two zircon grains (*A*) and (*B*) from sample 020. Both grains show fine prismatic zoning and a thin overgrowth that truncates internal zoning. *C*, Histogram of zircon $^{206}Pb/^{238}U$ ages. The χ^2 value of ~10 suggests that, for 29 degrees of freedom, the results are well described by a single Gaussian distribution and there is >99% probability that the sample represents a single age centered at 61.5 ± 2.0 Ma.

morphic quartz phenocrysts, others have idiomorphic K-feldspar, and others have plagioclase, biotite, and hornblende (sample 213). Hornblende from sample 213 was separated and purified to ~99% for purposes of a $^{40}Ar/^{39}Ar$ step heating experiment. Approximately 1% of the separate is composed of the fine-grained groundmass still attached to some of the hornblende phenocryst fragments. This groundmass appears to have suffered some alteration. At a crushed size of 85/150, mesh handpicking to purify the amphibole separate further was not possible.

Total release of argon from amphibole 213 was accomplished in 21 steps of 14 min heating duration each, with temperatures progressively increased over the course of the experiment, starting at 800°C and finishing with the final step at 1450°C. Table 5 gives the detailed results for each aliquot of gas evolved, and figure 7 shows the apparent age and K/Ca spectra. Analytical procedures are effectively the same as those described in Dunlap et al. (1995), except as noted below and footnoted in table 5. Correction factors $^{40}Ar/^{39}Ar_K$, $^{36}Ar/^{37}Ar_{Ca}$, and $^{39}Ar/^{37}Ar_{Ca}$ (table 5) were measured using a synthetic K-glass and pure CaF_2 included with the irradiation capsule. The results were used to correct the apparent ages for nucleogenic interferences on ^{40}Ar, ^{39}Ar, and ^{36}Ar.

Amphibole 213 exhibits a plateau-like pattern for steps 11 through 20 of the step heating experiment. The calculated age for this portion of the age spectrum, using size of step weighting, is 45.7 ± 0.8 (2σ) Ma, covering 84.1% of the total gas evolved. Note in figure 7 the correlation between elevated ages in the first 14% of gas release and elevated K/Ca. It is likely that this portion of gas release represents a mixture of gas from the amphibole and from the ~1% groundmass contaminant. Support for this hypothesis comes from the observation that feldspathic groundmass is likely to lose the vast majority of its argon by about 1140°C (this temperature is reached by step 10 and 14% of gas release). If this hypothesis is correct, then, considering the very small proportion of groundmass, the trapped argon within the groundmass must have a very high apparent age, perhaps because of recoil loss of ^{39}Ar from the very fine-grained material. An inverse isochron analysis of the data is consistent with our above interpretation of the plateau age. The isochron, which is heavily weighted by the larger gas fractions (fig. 8), indicates an age of 44.6 ± 0.7 Ma (1σ), with an intercept composition of $^{36}Ar/^{40}Ar$ = 305.8 ± 4.9 (1σ). Our preferred crystallization age for the sample is that of the plateau-like portion of the age spectrum, 45.7 ± 0.8 Ma (2σ).

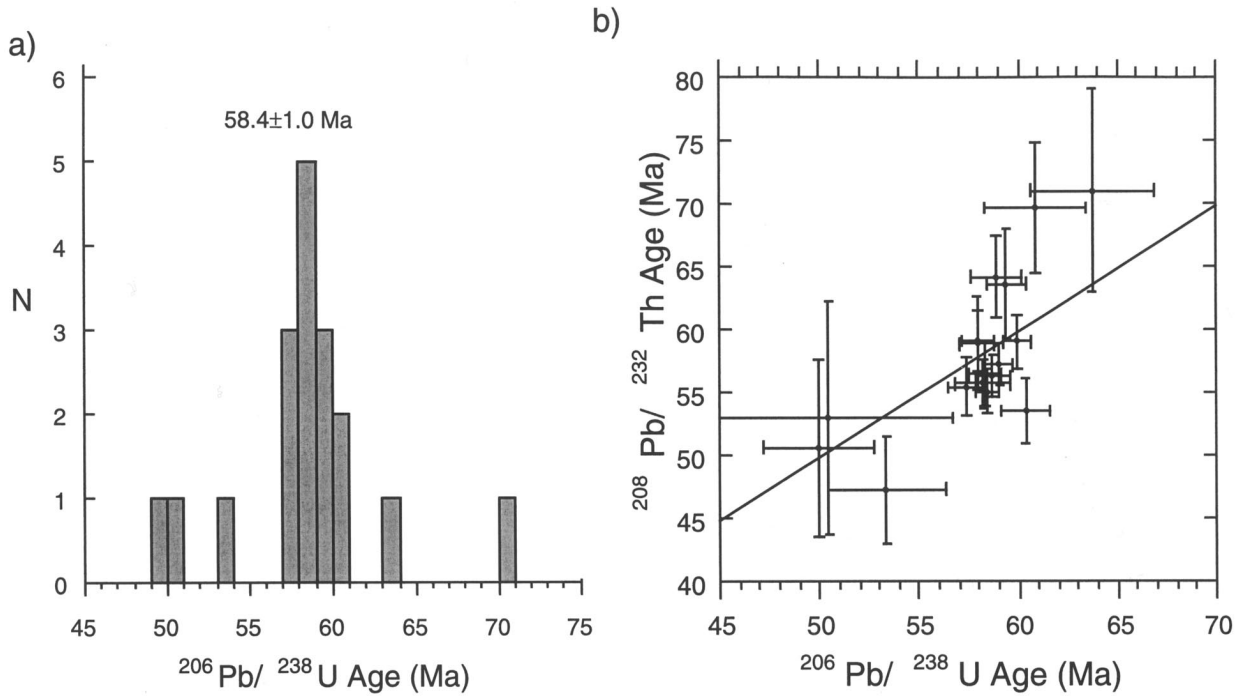

Figure 6. *a*, Histogram of zircon $^{206}Pb/^{238}U$ ages of sample 019 showing a well-defined single age centered at ca. 58.4 ± 1.0 Ma. *b*, Comparison between $^{206}Pb/^{238}U$ and $^{208}Pb/^{232}Th$ ages showing that the analyses yield the same age range but Th ages are more spread both above and below U ages. Note how the errors of the analyses that plot away from the main age group are much larger than those defining the main group.

The Thanglasgo Shear Zone—Batholith Deformation

Intense deformation developed since continental collision has partitioned to the volcanic and sedimentary rocks surrounding the Ladakh batholith with little deformation of the batholith rocks themselves. This is somewhat striking in view of the change in the main trend of the batholith in the vicinity of the Karakoram Fault (fig. 2). Batholith rocks on the northern side of the Ladakh Range, north of Leh, are generally undeformed. In the Thanglasgo Valley (north of Lasirmu La), there is a major shear zone a few kilometers wide (a minimum of 2 km), oriented N 24° W/90, parallel to the Karakoram Fault that outcrops 25 km to the east. Within this shear zone, the regional granodiorite is strongly deformed to mylonitic gneisses with narrow bands of mylonites. Small blocks of ultramylonites were found in the scree but were not observed in outcrop. Similar to the Karakoram Fault, mineral lineation in the TSZ plunges 20° NNW, and S-C fabric indicates a right-lateral sense of shear (fig. 9).

Quantitative indicators of the amount of displacement across the TSZ were not found. To the northwest the shear zone could not be followed because of border conflicts between Pakistan and India, to the southeast the prominent topographic lineament parallel to the TSZ vanishes, and the shear zone was not found along strike on the south side of the Ladakh Range. Instead, there is widespread, diffuse deformation of batholith rocks around Leh (shaded area in fig. 2). Despite the absence of markers, the width and intensity of deformation within the shear zone suggest that it may have accommodated significant dextral movement (of the order of tens of kilometers).

The similarity in orientation and sense of shear between the Karakoram Fault and TSZ suggests that they developed in response to the same straining. Recent work on the Karakoram Fault has constrained its initiation at less than ca. 15 Ma (Searle et al. 1998; Weinberg et al. 2000). This result, however, does not necessarily constrain the time of initiation of dextral shearing in northern Ladakh, since strain may have been taken up by other fault zones such as the TSZ. K-feldspar grains from a sample of mylonite gneiss from the shear zone (sample 413; ANU catalog 95413) north of the crest of the Ladakh Range were separated to help con-

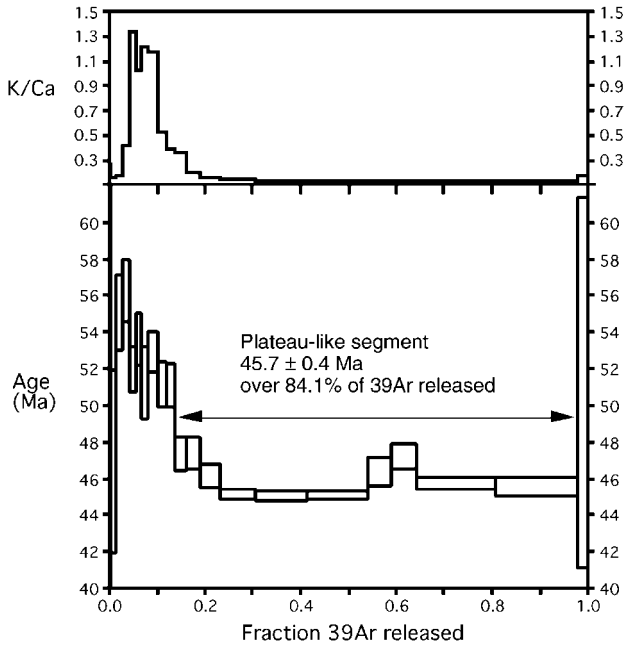

Figure 7. Age spectrum and K/Ca diagrams for the stepwise release of argon from sample 213 amphibole.

strain the timing of movement along the TSZ by means of $^{40}Ar/^{39}Ar$ step heating experiments.

Microstructures. The mylonitic gneiss sample 413 presents a fabric typical of deformation in the greenschist facies. Quartz is commonly recrystallized to fine polygonal grains (40–80 μm). Primary igneous biotite is bent and disaggregated and metamorphosed to chlorite. Cathodoluminescence (CL) images indicate that concentrations of fine grains of K-feldspar and plagioclase (<40 μm) lie in "pressure shadow" regions (under CL feldspar porphyroclasts and recrystallized tails luminesce in faint deep blue, whereas quartz does not luminesce); that is, the grains are concentrated in the foliation and areas adjacent to large porphyroclasts of original igneous feldspar grains. Feldspar grains are deformed by fracturing (fig. 9).

The combination of plastic deformation of quartz and of small feldspar grains and the growth of new white micas indicate that deformation occurred between ~300°C and 450°C (e.g., Hirth and Tullis 1992; Tullis and Yund 1987, 1992; Spear 1993). Thus, $^{40}Ar/^{39}Ar$ age gradients in K-feldspar porphyroclasts must record cooling and closure to loss of argon during greenschist facies shearing. Petrographic examination of the K-feldspar mineral separate that was dated indicates that it is composed primarily of porphyroclast cores (~95% by volume).

K-feldspar Thermochronology. In thermal modeling, effectively an interpretation, of $^{40}Ar/^{39}Ar$ step heating of a K-feldspar concentrate from sample 413 (table 6 and fig. 10), we interpret the results in terms of cooling through a closure temperature range of about 350°–150°C, the typical closure temperature window afforded by K-feldspar if simple diffusion theory is strictly applicable (for development of this method see Richter et al. 1991; Lovera et al. 1997). The analytical procedures were essentially the same as those used by Dunlap et al. (1995) at the Australian National University.

We assume that the granite crystallized at 60 Ma, but the modeling results are not sensitive to this assumption; we could have chosen 70 or 80 Ma without undue effect on our preferred model. The other obvious constraint on the cooling history is that the sample was exposed at the surface before the present day. No other assumptions have been imposed except for the main tenet of the modeling, that the degassing of argon from the sample in the laboratory has occurred by the same mechanism (volume diffusion) as the closure to argon loss during natural cooling. The modeling provides a nonunique continuous cooling path; however, the true thermal path experienced by the sample must fall within narrow limits if the assumption of volume diffusion is valid. The argon degassing results for sample 413 K-feldspars have been inverted into a time-temperature history following the method of Lovera et al. (1989). The multidiffusion domain method assumes that, in both the natural and laboratory situations, the loss or retention of radiogenic argon is from a number of noninteracting do-

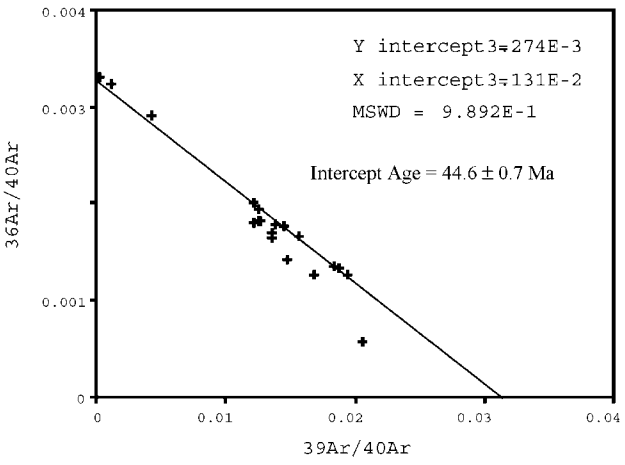

Figure 8. Inverse isochron diagram for the results of step heating of amphibole 213. Note the similarity in age between the intercept age in this figure and the plateau-like portion of figure 7.

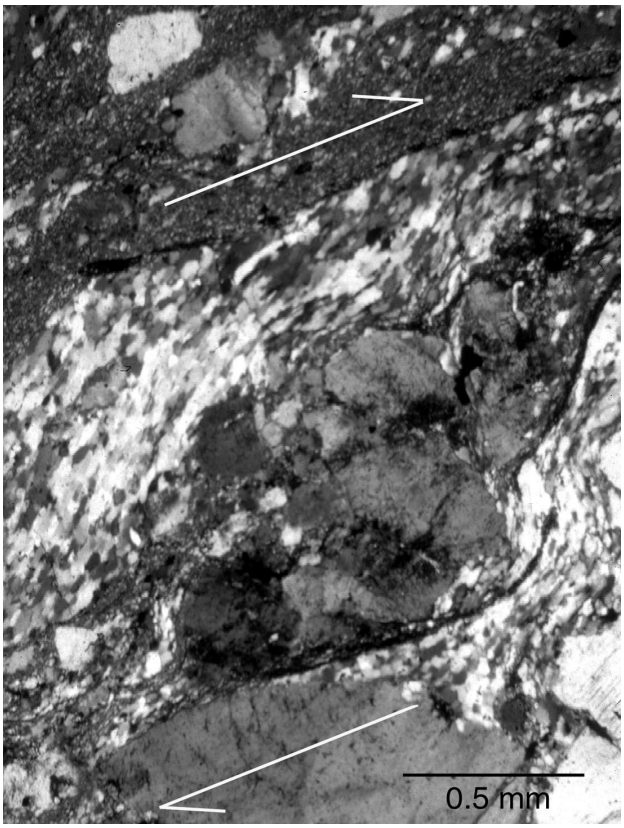

Figure 9. Photomicrograph of the Thanglasgo mylonite showing dextral sense of shear. Note how the feldspar porphyroclast is fractured in places and how it also developed very fine-grained tails (finer and darker than recrystallized quartz). The very fine-grained material at the top of the image is feldspar (determined by cathodoluminescence images), and the coarser, lighter recrystallized material is quartz.

mains of variable length scale (and/or diffusivity). For our purposes, a single activation energy and a slab geometry for volume diffusion of argon are assumed. The sample is dominated by one phase, so a single activation energy may be a reasonable assumption, although it is difficult to rule out multiple activation energies within a single phase. The slab geometry is consistent with the microstructure characteristic of K-feldspars that have suffered little postmagmatic alteration. The cooling history derived for K-feldspar sample 413 is not overly dependent on these assumptions (Lovera et al. 1997). The justification for the multidiffusion domain procedure (Lovera et al. 1997) is that K-feldspars commonly contain dramatic age gradients that cannot be produced by closure of a single domain to diffusive loss of argon (e.g., McDougall and Harrison 1988).

A multidiffusion domain solution (Lovera et al. 1989) has been calculated for the Arrhenius data using the time, temperature, and fraction of ^{39}Ar released during the degassing experiment (see table 6; fig. 10). Armed with this distribution of model diffusion length scales and the volume fractions of each length scale (also an output of the method; Lovera et al. 1989), the preferred thermal path was calculated by inputting trial thermal histories and minimizing the differences between the measured and modeled age spectra by manual iteration.

The age spectrum derived from detailed step heating of sample 413 K-feldspar (fig. 10*a*) indicates that the sample remained in the partial retention window for diffusive loss of argon subsequent to continent-continent collision at ~52 Ma; apparent ages range from 52 to 22 Ma. Although our preferred thermal path (fig. 10*d*) is nonunique, we prefer to model the cooling history of the sample 413 granitoid as one of continuous cooling (e.g., the sample is never reheated), which is consistent with the geology. Despite the nonuniqueness of the model, it is clear that deviations of a few tens of degrees from our preferred thermal path result in very poor fits to the data (a good fit is essentially continuous overlap between model and spectra measured in fig. 10*a*). For example, thermal histories hotter or colder (*dashed line* in fig. 10*d*) than the preferred one (*solid line* in fig. 10*d*) result in model fits (thin spectrum in fig. 10*a*) that deviate markedly from that measured in the laboratory ("Measured" spectrum in fig. 10*a*). We have assumed that the granite crystallized at 60 Ma, when the temperature was likely to be about 750°C. Initial closure of the largest domains of the K-feldspar must occur by 52 Ma and at ca. 300°C. This suggests quite rapid cooling from 60 to 52 Ma. Subsequent to 52 Ma, however, the model requires cooling at a rate of about 2°C/m.yr. The best fit is obtained if the cooling rate slows to 0°C before 22 Ma. The model ends at 22 Ma, at which time the temperature must be about 260 ± 20°C. After 22 Ma the cooling rate must increase if the sample is to reach 0°C at the present day.

As sample 413 comes from within a zone of significant shearing, we have considered the possibility that shear heating has affected the thermal history of the sample, and we provide eight thermal models that fit the data. However, the fact that the K-feldspar sample 126 of Dunlap et al. (1998) from the undeformed core of the batholith some 60 km along strike to the southeast yields an age spectrum essentially indistinguishable from that of sample 413 suggests that shear heating might have been unimportant.

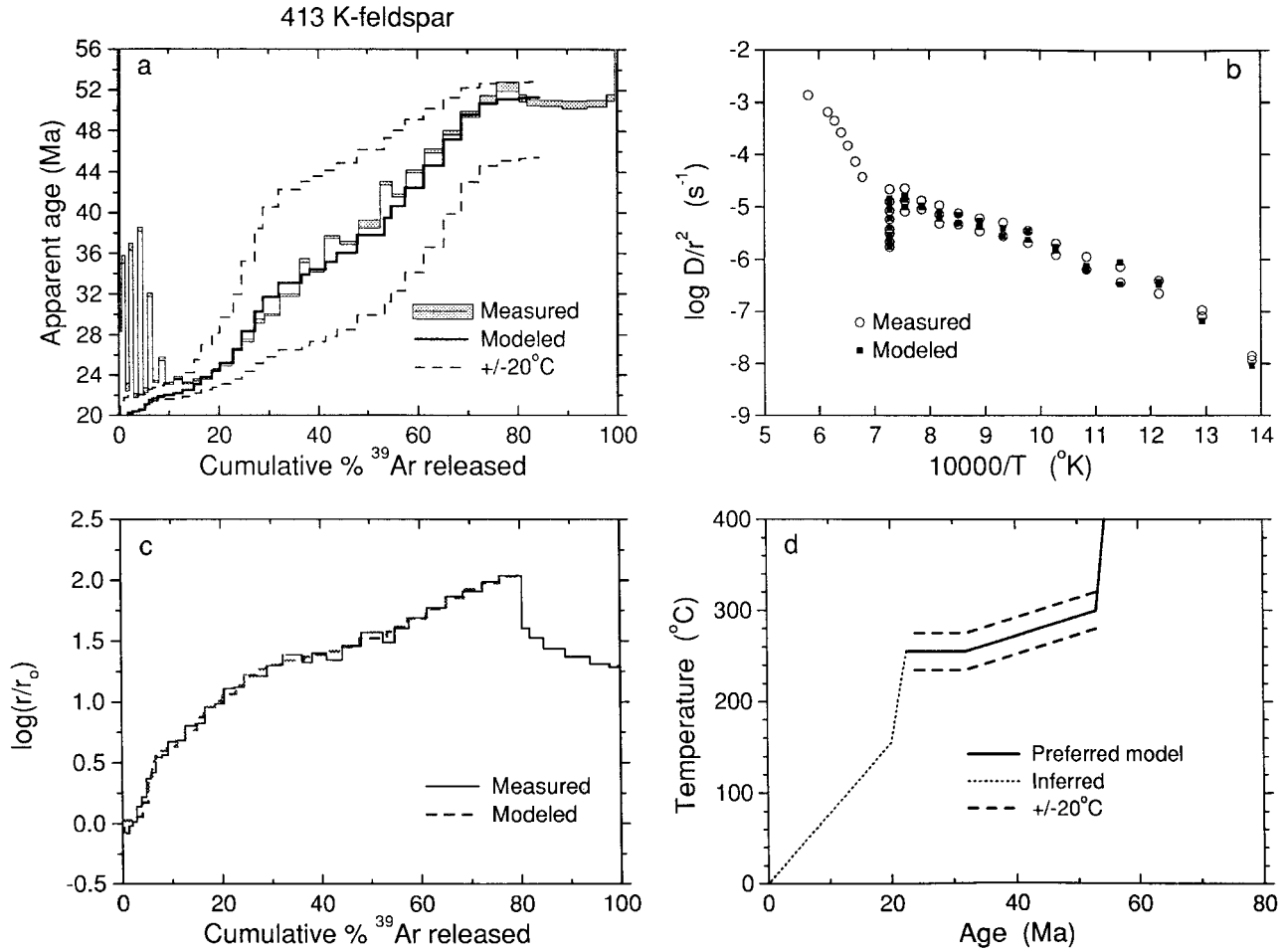

Figure 10. Results of thermal modeling of K-feldspars sample 413 from the Thanglasgo Shear Zone. *a*, Measured laboratory and best-fit model age spectra (*central curves*). The dashed spectra, above and below, illustrate the sensitivity of the model to increase/decrease in model temperatures by 20°C (see *d* for details). *b*, Thermal paths for shear-related reheating models. Eight solutions are shown, two each centered on times of 41, 31, 26, and 22 Ma. All eight models yield satisfactory fits such as that shown in the age spectrum diagram (*a*) to the left. *c*, Log r/r_o plot, shows increase in relative domain size as experiment progresses from left to right; see Lovera et al. (1989) for further details. *d*, Model thermal histories with solid line as the preferred model and thin lines representing models ±20°C. Solid lines show monotonically decreasing temperatures with time, a case that we argue is likely for the granite. Implicit in the analysis is that the thermal models in (*d*) are not valid before ~52 Ma, the oldest age step. In these models, initial crystallization of the grains is considered to have occurred at 60 Ma. Sample locality is shown in figure 3*A*.

To test the hypothesis of shear-related reheating, we have varied the timing of reheating, the magnitude of reheating, and the time scale of reheating. We have used a square pulse to simulate the reheating. Reheating must take place after ~52 Ma to have any affect on the age spectrum. Therefore, to study the timing of reheating, we imposed reheating pulses centered on 41, 31, 26, 22, 20, and 10 Ma. Reheating after about 22 Ma does not provide satisfactory fits to the data, so this possibility was ruled out. We used time scales of reheating (the time length of the square pulse) of 1 and 0.1 Ma. We believe that these time scales are about the shortest reasonable; anything shorter may not produce enough heat with displacement at tectonic rates (<10 cm/yr) over such a wide zone. The magnitudes of reheating required for good model fits are shown in figure 10*b* for both the 1-Ma and 0.1-Ma time scales (all eight models are shown; two models each centered on 22, 26, 31, and 41 Ma). Peak temperatures for the reheating range from 280°–390°C for square pulses of such short duration; it is obvious that pulses of longer duration require lower maximum temperatures for good fits.

In summary, the possibility of shear-related reheating leaves the timing of shearing in some doubt, in that it can take place at any time between ~52 and 22 Ma, but no later than that.

Interpretation. From our results, we expect sample 413 to have been at magmatic temperatures, well above the highest closure temperature of K-feldspar, at some time around 60–50 Ma. Our results indicate that after a period of rapid cooling, cooling slowed down. Subsequent to ~52 Ma the model requires slow cooling (~2°C/m.yr.) followed by a period of effectively no cooling until about 22 Ma for the synthetic age spectrum to match the laboratory-derived age spectrum. Deviations from this thermal path of as little as 20°C result in extremely poor model fits (fig. 10*a*). Thus, it is likely that the presently exposed level of the Ladakh Range at site 413 remained between 300°C and 260°C between 52 and 22 Ma.

The temperature at which the deformation took place is critical to our interpretation. Mica growth, plastic deformation of quartz grains, and the lack of pervasive plastic deformation in the feldspar grains constrain the temperature range during deformation to between 450° and 300°C. The argon system in K-feldspar grains of sample 413 start recording cooling when the sample reached 300°C. Thus, the bulk of shearing may have occurred before ca. 52 Ma as the rock cooled from its magmatic temperature. However, as the estimate of deformation temperature is inexact and because the sample cooled slowly, in our interpretation, across the $^{40}Ar/^{39}Ar$ window, we prefer the more conservative estimate that shearing occurred before closure of K-feldspar grains at ca. 22 Ma. Thus, we conclude that dextral shearing on the TSZ occurred at least 7 m.yr. before that on the <15-Ma Karakoram Fault.

Discussion

Schärer et al. (1984*a*) provided strong evidence of inheritance of radiogenic lead in their granite sample HB-87. SHRIMP age determinations here of older cores and rims of >50 zircons from three samples yielded individual ages between 72 and 48 Ma, all dating growth of the Ladakh batholith, and none representing older, prebatholith zircon cores. The lack of participation of older crust is further supported by O, Sr, and Sm-Nd isotopes. The age range obtained suggests that the belt was continuously active from at least ca. 70 to ca. 50 Ma, with no obvious age trend N-S across the batholith. More age determinations are required to answer the question posed by Schärer et al. (1984*a*) of whether or not the belt was active between the older mid-Cretaceous event dated near Kargil and the early Tertiary event dated here.

The sample 213 hornblende $^{40}Ar/^{39}Ar$ cooling age indicates that the Leh pluton cooled rapidly and that minor dike intrusions continued to penetrate the batholith to at least 46 ± 1 Ma. The $^{40}Ar/^{39}Ar$ and K-Ar studies of samples of the batholith published here and elsewhere indicate that temperatures <350°C were widespread over the presently exposed levels of the batholith by about 50 Ma. For example, the $^{40}Ar/^{39}Ar$ step heating experiment on K-feldspar sample 96-413 from the central core of the batholith indicates that temperatures of around ~350°C have not been exceeded since about 52 Ma. Similarly, K-feldspar sample 126 from Chang La (fig. 3*A*, E-SE of Leh; Dunlap et al. 1998) cooled to below ~350°C by 49 Ma. Finally, a K-Ar age of 48.7 ± 1.6 Ma was found for a sample of Shey granite (part of the Leh pluton) by Honegger et al. (1982). Thus, we conclude that the presently exposed levels of the Ladakh batholith have remained below 350°C since 49–52 Ma.

Comparison with the Kohistan Batholith. Dating Kohistan batholith rocks is restricted to Rb-Sr ages and $^{40}Ar/^{39}Ar$ cooling ages (e.g., Petterson and Windley 1985; Treloar et al. 1989; Zeitler et al. 1989; George et al. 1993). Whereas the oldest rocks dated in Kohistan coincide with the oldest in Ladakh at ca. 102 Ma, magmatism in Kohistan seems to have continued longer. In contrast to Ladakh, a young, postcollisional granitic phase intruded the Kohistan batholith and surroundings (Petterson and Windley 1985; George et al. 1993). These are biotite granite sheets (the Confluence granites) and muscovite granite sheets (the Parri granite sheets), both with a strong mantle Sr and Nd isotopic signature (George et al. 1993). The sheared versions of the Parri granites, cropping out close to the Nanga Parbat-Haramosh Massif, have a pronounced increase in initial Sr ratios and decrease in ϵ_{Nd}, interpreted by George et al. (1993) as resulting from subsolidus fluid infiltration or assimilation of crustal material. George et al. (1993) determined a Rb-Sr 10-point errorchron for the Confluence granites, yielding an age of 49 ± 11 Ma. For the Parri granites, they found an errorchron age of 26 ± 1 Ma. In Ladakh, such young granites have not been confirmed, though tourmaline granite dikes at Chumathang (east of Leh along the Indus Valley; J. Dunlap, pers. observ.), and garnet-bearing rhyolites near Teah (west of Leh; Raz and Honegger 1989; R. Weinberg, pers. observ.) are possible candidates.

Assuming that the errorchron ages of these granites are representative of their crystallization age,

magmatism in Kohistan did not halt entirely after continental collision. Petterson et al. (1993) concluded that these granites resulted from the remelting of the Kohistan plutons. We contend however that these younger granites are not a result of melting related to subduction of an oceanic crust under an island arc but, rather, result from the evolution of the continental collision. This hypothesis is supported by the increased crustal signature in sheared granites in the vicinity of the Nanga Parbat-Haramosh Massif (George et al. 1993), suggesting that rocks originated in the Indian continental crust cropping out in the massif played a significant role in the origin of these younger magmas.

Timing of Collision. Rowley (1996) and Treloar (1997) have summarized available information concerning timing of continental collision and discussed the implications of each different possibility. Although there are indications that collision may have initiated as early as the Cretaceous-Tertiary boundary (Klootwijk et al. 1992; Beck et al. 1995), there is strong evidence that in the NW Himalayas collision occurred in the Ypresian, roughly 52 –50 Ma (Garzanti et al. 1987; Bossart and Ottiger 1989; Pivnik and Wells 1996; Rowley 1996). In addition, Patriat and Achache (1984) demonstrated a dramatic slowing down and temporary erratic migration direction of the Indian plate between 52 and 50 Ma, which they interpreted to be a result of collision.

Collision caused the end of the subduction process that drove magmatism in the Ladakh batholith. Thus, it is possible that the end of calc-alkaline magmatism in the Ladakh batholith provides an indirect way of dating collision. Since there may be an inertia in the process, the end of magmatism in the overriding plate may occur somewhat later than the actual collision. Comparison between the time of collision derived from sedimentary sequences with that provided by the batholith should help us constrain the possible time delay between the initiation of collision and the end of magmatism. Because the Leh pluton is the youngest major intrusive phase in the area and was followed by generalized cooling of the batholith and minor subvolcanic dike intrusions (the 45.7 ± 0.8-Ma [2σ] andesite Phyang dikes), we suggest that its 49.8 ± 0.8-Ma crystallization age closely marks the disruption of the magmatic system resulting from the disruption of the subduction of Tethys oceanic lithosphere caused by continental collision. Because of the possible time lag between disruption of the subducting plate and the end of magmatism in the overriding plate, the age of the Leh pluton must be taken as an upper bound for the timing of collision. We note, however, that this age is very close to the age of collision determined from sedimentary sequences and conclude that the inertia of the magmatic system is minimal and that it responded immediately, within error, to collision.

Schärer et al. (1984*b*) dated crystallization of granodiorites at Qushui, along the eastward continuation of the Trans-Himalayan batholith near Lhasa, and found concordant U-Pb ages of ca. 41 Ma. They used these results to argue that collision in the Lhasa-Xigaze sector of the collision must have postdated granite emplacement and therefore must have occurred after Lutetian time. Comparison with the Leh pluton and Ladakh batholith, in general, suggests eastward younging of collision.

Remelting of Early Batholith Intrusions. The main process believed to give rise to crustal growth in modern plate tectonic settings, which has also been used to explain early Archean crustal growth, is a two-stage melting process occurring mostly along destructive plate margins (e.g., Kay and Mahlburg-Kay 1991). This process is thought to produce large calc-alkaline, Andean-type batholiths and is characterized by the addition of basaltic magmas to the crust, followed by their later remelting to produce evolved melts of average crustal (andesitic) composition (e.g., Gromet and Silver 1987). These authors argued that remelting of deeply emplaced magmas leads to the high volumes of granitoids found in continental igneous belts, as opposed to island arcs where shallow level mantle magmas do not undergo remelting, and where small volumes of granitoids are directly derived from the crystal fractionation of basalts. It is generally agreed today that Andean-type magmas are derived in part from the remelting of more primitive mantle-derived magmatic rocks (Pitcher 1993). Closer to Ladakh, Petterson et al. (1993) concluded that the Kohistan batholith evolved through the remelting of recently formed arc crust in addition to new mantle-derived magmas.

The age of the two Gyamsa events (crystallization of the quartz-diorite and its later remelting) are not clearly defined by the zircon ages. Nevertheless, the results suggest that the quartz-diorite crystallized and remelted, possibly because of fluctuations in pressure or temperature, during batholith growth, between ca. 70 and 50 Ma. The Leh quartz-diorite, in contrast, has two main zircon morphologies yielding two different but closely spaced ages. The Leh quartz-diorite crystallized at 49.8 ± 0.8 Ma and inherited zircons from its source, an earlier plutonic rock that crystallized only ca. 8 m.yr. before. Together, these results suggest that the remelting of early batholith igneous

rocks to originate younger melts played an important role in the evolution of the batholith and explain the origin of large volumes of granitoids with a strong mantle signature (e.g., Gromet and Silver 1987). This process leads to crustal growth and temporal evolution toward increasingly more evolved felsic magmas, as observed in several large Andean batholiths such as the Peruvian Andes (Pitcher 1993), the Sierra Nevada (Bateman 1983), and the Kohistan (Petterson and Windley 1985) and Ladakh batholiths (Raz and Honegger 1989).

Internal Deformation. Dextral shearing along the TSZ was able to accommodate some of the internal deformation of the Ladakh batholith implied by the change in trend in the vicinity of the Karakoram Fault. We predict that further mapping of the batholith east of Leh will reveal other structures that contributed to rotating the batholith. Similarly, we predict that the Karakoram batholith, north of the fault, may have been internally deformed. Our preliminary investigations there revealed weak, but pervasive, deformation.

Relative Displacement between India and the Tibetan Plateau. Since the Tibetan Plateau is thought to be bounded on the southwest by the Karakoram Fault, deformation along and around the fault are fundamental to our understanding of the tectonic development of the plateau. Searle et al. (1998) demonstrated relatively small displacement across the Karakoram Fault (ca. 150 km). Our findings suggest that the Karakoram Fault is the most recent and most obvious expression of dextral shearing in Ladakh. Dextral shearing on the TSZ started at least 7 m.yr. before that along the Karakoram Fault. The bending of the main trend of the Ladakh and Karakoram batholiths near the Karakoram Fault are expressions of dextral shearing over a zone at least 100 km wide. The total relative displacement between the Tibetan Plateau and India has to be measured over that width and may be larger than the ca. 150 km measured across the Karakoram Fault alone. Large uncertainties on the total amount of dextral displacement in northern Ladakh result from the difficulty in reconstructing the preshearing shape of the Ladakh (Transhimalayan) batholith because of the present lack of detailed maps of the batholith on either side of the fault.

Conclusions

The Ladakh batholith around Leh grew by the addition of several magma pulses crystallized between ca. 70 and 50 Ma. Inherited zircons only a few million years older than the crystallization age of the magma, together with field relations, suggest that the remelting of earlier plutons to produce younger ones seems to have played a fundamental role in the evolution of the batholith and explains the origin of large volumes of granitoids with a strong mantle signature. The 49.8 ± 0.8-Ma Leh pluton was most likely the last major magma pulse in the batholith. Its emplacement was followed by rapid cooling at the presently exposed levels to below 350°C, and shortly thereafter by minor subvolcanic dike intrusions at 45.7 ± 0.8 Ma. The main episode of batholith growth ended at the time of continental collision, closely dated by Leh pluton rocks. Comparison between the Ladakh batholith and the Qushui granodiorites near Lhasa suggests that collision started later eastward. Dextral shearing parallel to the N 30° E–striking Karakoram Fault started at least 7 m.yr. before this fault, as revealed by our study of the TSZ. Over time, dextral shearing affected a band at least 100 km wide, causing reorientation of both the Ladakh and the Karakoram batholiths immediately north and south of the Karakoram Fault in northern Ladakh. The total dextral displacement across this broad zone could be up to 300 km.

ACKNOWLEDGMENTS

R. F. Weinberg thanks Bill Compston for access to the SHRIMP and assistance throughout. We thank Paul Sylvester for chemical analyses. We also appreciate the support of D. Green, I. McDougall, and R. Griffith and thank B. Kamber for comments on an early version of the text and for help with the analysis of published isotope data. We also thank Peter Treloar, An Yin, and Clark Burchfiel for careful reviews. This work was partly supported by the EC grant ERBFMBICT960583, the Australian Nuclear Science and Technology Organization, and the Australian Institute of Nuclear Science and Engineering.

REFERENCES CITED

Allègre, C. J., and Ben Othman, D. 1980. Nd-Sr isotopic relationship in granitoid rocks and continental crust development: a chemical approach to orogenesis. Nature 286:335–342.

Allègre, C. J.; Hart, S. R.; and Minster, J. F. 1983. Chemical structure and evolution of the mantle and continents determined by inversion of Nd and Sr isotopic data. II. Numerical experiments and discussion. Earth Planet. Sci. Lett. 66:191–213.

Bateman, P. C. 1983. A summary of critical relations in the central part of the Sierra Nevada batholith, California, U.S.A. Geol. Soc. Am. Mem. 159:241–254.

Beck, R. A.; Burbank, D. W.; Sercombe, W. J.; Riley, G. W.; Barndt, J. K.; Berry, J. R.; Afzal, J.; et al.1995. Stratigraphic evidence for an early collision between northwest India and Asia. Nature 373:55–58.

Blattner, P.; Dietrich, V.; and Gansser, A. 1983. Contrasting ^{18}O enrichment and origins of High Himalayan and Transhimalayan intrusives. Earth Planet. Sci. Lett. 65: 276–286.

Bossart, P., and Ottiger, R. 1989. Rocks of the Muree formation in northern Pakistan: indicators of a descending foreland basin of late Paleocene to middle Eocene age. Eclogae Geol. Helv. 82:133–165.

Claoué-Long, J. C.; Compston, W.; Roberts, J.; and Fanning, C. M. 1995. Two Carboniferous ages: a comparison of SHRIMP zircon dating with conventional zircon ages and $^{40}Ar/^{39}Ar$ analysis. *In* Berggren, W. A.; Kent, D. V.; Aubry, M.-P.; and Hardenbol, J., eds. Geochronology time scales and global stratigraphic correlation. Soc. Sediment. Geol. Spec. Publ. 3-21.

Debon, F.; Le Fort, P.; Sheppard, S. M.; and Sonet, J. 1986. The four plutonic belts of the Transhimalaya-Himalaya: a chemical, mineralogical, isotopic, and chronological synthesis along a Tibet-Nepal section. J. Petrol. 27:219–250.

De Terra, H. 1934. Physiographic results of a recent survey in Little Tibet. Geog. Rev. 24:12–41.

Dunlap, W. J.; Teyssier, C.; McDougall, I.; and Baldwin, S. 1995. Thermal and structural evolution of the intracratonic Arltunga Nappe Complex, central Australia. Tectonics 14:1182–1204.

Dunlap, W. J.; Weinberg, R. F.; and Searle, M. P. 1998. Karakoram metamorphic rocks cool in two phases. J. Geol. Soc. Lond. 155:903–912.

Garzanti, E.; Baud, A.; and Mascle, G. 1987. Sedimentary record of the northward flight on India and its collision with Eurasia (Ladakh, Himalaya, India). Geodin. Acta 1:297–312.

George, M. T.; Harris, N.; and Butler, R. W. H. 1993. The tectonic implications of contrasting granite magmatism between the Kohistan island arc and the Nanga Parbat-Haramosh Massif, Pakistan Himalaya. *In* Treloar, P. J., and Searle, M. P., eds. Himalayan tectonics. Geol. Soc. Lond. Spec. Publ. 74:173–191.

Gromet, L. P., and Silver, L. T. 1987. REE variations across the Peninsular Ranges Batholith: implications for batholithic petrogenesis and crustal growth in magmatic arcs. J. Petrol. 28:75–125.

Hirth, G., and Tullis, J. 1992. Dislocation creep regimes in quartz aggregates. J. Struct. Geol. 14:145–159.

Honegger, K.; Dietrich, V.; Frank, W.; Gansser, A.; Thöni, M.; and Trommsdorff, V. 1982. Magmatism and metamorphism in the Ladakh Himalayas (the Indus-Tsangpo suture zone). Earth Planet. Sci. Lett. 60: 253–292.

Kay, R. W., and Mahlburg-Kay, S. 1991. Creation and destruction of lower continental crust. Geol. Rundsch. 80:259–278.

Klootwijk, C. T.; Gee, J. S.; Pierce, J. W.; Smith, G. M.; and McFadden, P. L. 1992. An early India-Asia contact: paleomagnetic constraints from Ninetyeast Ridge, ODP Leg 121. Geology 20:395–398.

Lovera, O. M.; Grove, M.; Harrison, T. M.; and Mahon, K. I. 1997. Systematic analysis of K-feldspar $^{40}Ar/^{39}Ar$ step heating results. I. Significance of activation energy determinations. Geochim. Cosmochim. Acta 61: 3171–3192.

Lovera, O. M.; Richter, F. M; and Harrison, T. M. 1989. The $^{40}Ar/^{39}Ar$ thermochronometry for slowly cooled samples having a distribution of diffusion domain sizes. J. Geophys. Res. 94:17,917–17,935.

McDougall, I., and Harrison, T. M. 1988. Geochronology and thermochronology by the $^{40}Ar/^{39}Ar$ method. New York, Oxford University Press, 212 p.

Patriat, P., and Achache, J. 1984. India-Eurasia collision chronology has implication for crustal shortening and driving mechanisms of plates. Nature 311:615–621.

Petterson, M. G.; Crawford, M. B.; and Windley, B. F. 1993. Petrogenetic implications of neodymium isotope data from the Kohistan batholith, North Pakistan. J. Geol. Soc. Lond. 150:125–129.

Petterson, M. G., and Windley, B. F. 1985. Rb-Sr dating of the Kohistan arc-batholith in the Trans-Himalaya of north Pakistan, and tectonic implications. Earth Planet. Sci. Lett. 74:45–57.

———. 1991. Changing source regions of magmas and crustal growth in the Trans-Himalayas: evidence from the Chalt volcanics and Kohistan batholith, Kohistan, northern Pakistan. Earth Planet. Sci. Lett. 102: 326–341.

Pitcher, W. S. 1993. The nature and origin of granite. London, Chapman & Hall, p. 321.

Pivnik, D. A., and Wells, N. A. 1996. The transition from Tethys to the Himalaya as recorded in NW Pakistan. Geol. Soc. Am. Bull. 108:1295–1313.

Raz, U., and Honegger, K. 1989. Magmatic and tectonic evolution of the Ladakh Block from field studies. Tectonophysics 161:107–118.

Richter, F. M.; Lovera, O. M.; Harrison, T. M.; and Copeland, P. 1991. Tibetan tectonics from $^{40}Ar/^{39}Ar$ analysis

of a single K-feldspar sample. Earth Planet. Sci. Lett. 105:266–278.

Rowley, D. B. 1996. Age of initiation of collision between India and Asia: a review of stratigraphic data. Earth Planet. Sci. Lett. 145:1–13.

Schärer, U.; Hamet, J.; and Allegre, C. J. 1984*a*. The Transhimalaya (Gangdes) plutonism in the Ladakh region: U-Pb and Rb-Sr study. Earth Planet. Sci. Lett. 67:327–339.

Schärer, U.; Xu, R.-H.; and Allègre, C. J. 1984*b*. U-Pb geochronology of Gangdese (Transhimalaya) plutonism in the Lhasa-Xigatze region, Tibet. Earth Planet. Sci. Lett. 69:311–320.

Searle, M. P.; Weinberg, R. F.; and Dunlap, W. J. 1998. Tranpressional tectonics along the Karakoram Fault Zone, northern Ladakh. *In* Holdsworth, R. E., and Strachan, R. A., eds. Continental transpression and transtentional tectonics. Geol. Soc. Lond. Spec. Publ. 135, p. 307–326.

Spear, F. S. 1993. Metamorphic phase equilibria and pressure-temperature-time paths. Mineral. Soc. Am. Monogr. Chelsea, Mich., Bookcrafters, 799 p.

Srimal, N. 1986. Geology and oxygen and $^{40}Ar/^{39}Ar$ isotopic study of India-Asia collision in the Ladakh and Karakoram Himalaya, NW India. Ph.D. dissertation, University of Rochester.

Srimal, N.; Basu, A. R.; and Kyser, T. K. 1987. Tectonic inferences from oxygen isotopes in volcano-plutonic complexes of the India-Asia collision zone, NW India. Tectonics 6:261–273.

Tapponnier, P.; Peltzer, G.; LeDain, A. Y.; Armijo, R.; and Cobbold, P. R. 1982. Propagating extrusion tectonics in Asia: new insights from simple experiments with plasticine. Geology 10:611–616.

Treloar, P. 1997. Thermal controls on early-Tertiary, short-lived, rapid regional metamorphism in the NW Himalaya, Pakistan. Tectonophysics 273:77–104.

Treloar, P. J.; Guise, P. G.; Coward, M. P.; Searle, M. P.; Windley, B. F.; Petterson, M. G.; Jan, M. Q.; and Luff, I. W. 1989. K-Ar and Ar-Ar geochronology of the Himalayan collision in NW Pakistan: constraints on the timing of suturing, deformation, metamorphism and uplift. Tectonics 8:881–909.

Tullis, J., and Yund, R. A. 1987. Transition from cataclastic flow to dislocation creep of feldspar: mechanisms and microstructures. Geology 15:606–609.

———. 1992. The brittle-ductile transition in feldspar aggregates: an experimental study. *In* Evans, B., and Wong, T. F., eds. Fault mechanics and transport properties of rocks. New York, Academic Press, p. 89–117.

Weinberg, R. F. 1997. The disruption of a diorite magma pool by intruding granite: the Sobu body, Ladakh Batholith, Indian Himalayas. J. Geol. 105:87–98.

Weinberg, R. F.; Dunlap, W. J.; and Whitehouse, M. 2000. New field, structural and geochronological data from the Shyok and Nubra valleys, northern Ladakh: linking Kohistan to Tibet. *In* Khan, M. A.; Jan, M. Q.; Treloar, P. J.; and Searle, M. P., eds. Tectonics of Western Himalaya and Karakoram. Geol. Soc. Lond. Spec. Publ. 170, p. 253–275.

Zeitler, P. K.; Sutter, J. F.; Williams, I. S.; Zartman, R.; and Tahirkeli, R. A. K. 1989. Geochronology and temperature history of the Nanga Parbat–Haramosh Massif, Pakistan. Geol. Soc. Am. Spec. Publ. 232:1–22.